Chapter 3 Time-Dependence and Shocks

None of the hydraulically-driven oceanic or atmospheric flows discussed in the introduction to this book are steady, and very few are approximately so. A striking example of unsteadiness was discovered by Worthington (1969) who in 1967 placed an array of 30 moored current meters in the Denmark Strait in order to measure the deep velocities of the overflow. When Worthington returned a year later he found that all but one of the instruments had been destroyed or could not be recovered. The surviving current meter showed a history of rapid velocity fluctuations ranging from near zero to 2m/s, most likely due to the meandering of the edge of the jet-like overflow back and forth across the instrument.

How applicable are the steady models of Chapters 1 and 2 to such flows? The answer to this question depends on how rapid the time fluctuations are. A rough measure of rapidity is the ratio of the free response time of the flow over the topographic feature to the characteristic time scale T_u of the unsteady motions. The response time is a measure of long it would take the steady flow to adjust to a sudden change in conditions. It is roughly the length L of the topographic feature divided by the characteristic speed c_- of a wave propagating upstream. The importance of time-dependence is thus measured by

$$L/(c_- T_u)$$

If $L/(c_- T_u) \ll 1$, the response of the flow is instantaneous compared to the observed period of fluctuations and the flow may be considered essentially steady. Although the flow is evolving, the time-dependence is parametric and local time derivatives need not be considered in the computation of the flow at any particular instant (see Exercise 1). If $L/(c_- T_u)=O(1)$ then the time dependence is dynamically important and local time derivatives should be retained. This last situation occurs in many oceanographically important straits where steady theory has traditionally been applied. For example, the Bab al Mandab (the strait connecting the Indian Ocean with the Red Sea) is about 200km in length and is subject to tides with a dominant period (T_u) of about 12 *hr*. The typical speed c_- of the first internal gravity wave in the strait is typically $1 m/s$ or less giving a travel time of at least $55 hr$. With these numbers $L/(c_- T_u) \cong 4.6$ and the flow must be considered dynamically unsteady. Even if the length of the sill ($\cong$40km) is used in place of the total strait length, $L/(c_- T_u)$ remains O(1).

Attempting to understand the hydraulics of flows undergoing continuous time variations has proven to be difficult and frustrating. The applicability of concepts such as hydraulic control and upstream influence in these situations is not well understood, even in the simplest cases. To gain ground, past investigators have concentrated efforts on initial-value problems in which the evolution beginning with some simple and intuitively desirable initial state leads to the establishment of a steady flow. Such models

help one to understand how steady solutions are established, how upstream influence is exercised, and why hydraulically controlled states are sometimes preferred over states that lack control. Initial-value experiments can also provide a first step towards understanding flows that are subject to continuously time-varying forcing, such as tidal forcing. One might think of continuous time variations as a sequence of initial value problems. Finally, initial-value problems often provide a convenient setting for the study of rotating shocks, which arise as the result of nonlinear wave steepening.

In this chapter we shall consider two-initial value problems, both grounded in classical fluid mechanics. The first is a rotating version of the dam-break problem (Sections 1.2 and 1.3) carried out in channel geometry. Also referred to as *Rossby adjustment in a channel* this problem has received the attention of a number of authors. The second problem has received less attention but is directly related to the models of sill flows discussed in Chapter 2. It is a rotating version of Long's experiment, in which an obstacle is placed in the path of a steady stream in a rotating channel. Hydraulic jumps, bores and other rotating shocks appear in both of these problems and the final sections of the chapter are devoted to a discussion of these objects.

3.1 Linear Rossby Adjustment in a Channel.

The Rossby adjustment problem in a channel belongs to a group of classical initial value problems that includes dam break and the lock exchange flows. The linear version of the problem was first solved by Gill (1976). Following the nondimensional notation and conventions introduced in Chapter 2, consider a rotating channel with sidewalls at $x=\pm w/2$ and a barrier at $y=0$. As shown in Figure 3.1.1a, the barrier separates stagnant fluid with uniform depth $d=1+a$ in ($y<0$) from depth $1-a$ in ($y>0$). At $t=0$ the barrier is removed allowing the deeper fluid to spill forwards. If $a<<1$ the shallow water equations can be linearized and solved for the subsequent evolution.

Assuming $a<<1$, we first expand the velocity and depth fields as

$$u = au^{(o)} + a^2 u^{(1)} + \cdots$$
$$v = av^{(o)} + a^2 v^{(1)} + \cdots$$
$$d = 1 + a\eta^{(o)} + a^2 \eta^{(1)} + \cdots$$

and substitute these expansions into the full shallow water equations. Because of the abrupt nature of the initial conditions, the semigeostrophic approximation will fail, at least in the vicinity of $y=0$ for small t. We therefore set $\delta=W/L=1$. With this minor change the equations governing the lowest order fields are just the linear shallow water equations (2.1.20-2.1.22) with $\delta=1$, or

$$\frac{\partial u}{\partial t} - v = -\frac{\partial \eta}{\partial x}, \tag{3.1.1}$$

$$\frac{\partial v}{\partial t} + u = -\frac{\partial \eta}{\partial y}, \tag{3.1.2}$$

and

$$\frac{\partial \eta}{\partial t} + \frac{\partial u}{\partial x} + \frac{\partial v}{\partial y} = 0 \tag{3.1.3}$$

Note that the $(\,)^{(o)}$ notation has been dropped.

The initial conditions are given by

$$\eta(x, y, 0) = \eta_o = -\mathrm{sgn}(y) \tag{3.1.4}$$

and $u(x, y, 0) = v(x, y, 0) = 0$. The boundary conditions are

$$u(\pm \tfrac{1}{2} w, y, t) = 0 \tag{3.1.5}$$

The linearized statement of potential vorticity conservation (see 2.1.23) for this case is

$$\frac{\partial v}{\partial x} - \frac{\partial u}{\partial y} - \eta = -\eta_o \qquad (3.1.6)$$

The linearized potential vorticity $\frac{\partial v}{\partial x} - \frac{\partial u}{\partial y} - \eta$ is thus conserved at each (x,y), rather than following a fluid element. 'Forward' points (with $y>0$) thus maintain higher potential vorticity than locations with $y<0$. The variables u and v may be eliminated from (3.1.6), resulting in a single equation for η:

$$\frac{\partial^2 \eta}{\partial^2 t^2} - \frac{\partial^2 \eta}{\partial^2 x^2} - \frac{\partial^2 \eta}{\partial^2 y^2} + \eta = \eta_o . \qquad (3.1.7)$$

(also see 2.1.24).

It will also be of interest to calculate the energy of the solution, and an expression of the linearized energy may be obtained by taking $u \times (3.1.1) + v \times (3.1.2) + \eta \times (3.1.3)$, resulting in

$$\frac{\partial}{\partial t}\left(\frac{u^2 + v^2 + \eta^2}{2} \right) = -\nabla \cdot (\mathbf{u}\eta) \qquad (3.1.8)$$

The left hand term is clearly the time rate of change of the kinetic plus potential energy at a point, whereas the left hand term can be interpreted as the divergence of an energy flux.

(a) The Rossby adjustment in an infinite domain.

Solving the full problem described above is technically involved and it is helpful to first consider the special limit of an infinite domain ($-\infty<x<\infty$). This limiting case is the classical 'geostrophic adjustment' problem considered by Rossby (1937, 1938). Since the initial conditions are independent of y and since the governing equation contains no x-dependent forcing terms, it follows that $\partial / \partial x = 0$ for all time. This fundamental simplification rules out Kelvin waves.

Another simplification recognized by Rossby is that potential vorticity conservation allows the asymptotic ($t\rightarrow\infty$) solution to be predicted without the need to calculate the time evolution. Assuming this state to be steady, (3.1.7) reduces to

$$\frac{\partial^2 \eta_\infty}{\partial y^2} - \eta_\infty = -\eta_o = \mathrm{sgn}(y) \qquad (3.1.9)$$

Of course, $\eta_\infty = \eta_o$ is a possible solution to this equation, provided that one is willing to overlook the singularity at *y*=0. However, we anticipate that the true asymptotic solution will be continuous in *y* at all points. [This expectation can be made rigorous by replacing the initial discontinuity in depth by an abrupt but continuous transition.] Granted the continuity of η_∞ at *y*=0, it follows from integration of (3.1.9) over a small interval about *y*=0 that $\partial\eta_\infty / \partial y$ must also be continuous there. With these provisos, the solution to (3.1.9) becomes

$$\eta_\infty = \begin{cases} -1 + e^{-y} & (y > 0) \\ 1 - e^{y} & (y < 0) \end{cases},$$

while the corresponding geostrophically balanced velocity is

$$u_\infty = -\frac{\partial \eta_\infty}{\partial y} = e^{-|y|}.$$

As shown in Figures 3.1.1b and 3.1.1c, this solution consists of a cusped jet centered at *y*=0 and moving in the positive-*x* direction. In contrast to the nonrotating version of this problem (Section 1.2), where the final flow is uniform and in the *y*-direction, the final flow here is parallel to the initial step. Another significant difference can be identified by computation of the total energy of the asymptotic state and comparing it with the initial energy. Integrating (3.1.8) over $0<t<\infty$ and over a long interval [-*L*,*L*] in the *y*-direction leads to

$$\tfrac{1}{2}\int_{-L}^{L} (\eta_o^2 - \eta_\infty^2 - u_\infty^2) dy = 1 = -\int_0^\infty [v\,\eta]_{y=-L}^{y=L} dt \qquad (3.1.10)$$

The left-hand term is the difference between the energies (per unit *x*) of the initial and asymptotic states. By direct calculation this difference is unity. Thus the asymptotic state contains one unit of energy less that the initial state. This deficit is due to the radiation of energy towards ± by Poincaré waves, as measured by the final term in (3.1.10). We next calculate these transient terms.

For reasons that will prove advantageous in our treatment of the channel geometry, we will solve for the transient part of the solution in terms of the variable *u*, rather than *y*. A single equation for the former may be obtained by eliminating *v* and η from (3.1.6) (also see exercise 2 of Section 2.1). The result is

$$\frac{\partial^2 u}{\partial^2 t^2} - \frac{\partial^2 u}{\partial^2 y^2} - \frac{\partial^2 u}{\partial^2 x^2} + u = -\frac{\partial \eta_o}{\partial y} = 2\delta(y), \qquad (3.1.11)$$

and we again take $\partial / \partial x = 0$.

Next, let $u = u_T + u_\infty = u_T + e^{-|y|}$ where u_T denotes the transient part of the solution. It follows that

$$\frac{\partial^2 u_T}{\partial^2 t^2} - \frac{\partial^2 u_T}{\partial^2 y^2} + u_T = 0, \tag{3.1.12}$$

$$u_T(y,0) = -e^{-|y|}, \tag{3.1.13}$$

and

$$\frac{\partial u_T}{\partial t}(y,0) = 0. \tag{3.1.14}$$

where the last relation follows from (3.1.1).

Since $u_T(y,0)$ is even in y and since (3.1.12) has $\pm y$ symmetry, $u_T(y,t)$ must also be even. We therefore seek a solution in the form of a Fourier cosine integral:

$$u_T(y,t) = \int_0^\infty \hat{u}_T(l,t)\cos(ly)\,dl \tag{3.1.15}$$

Taking the Fourier transform $\hat{f}(l) = \frac{1}{\pi}\int_{-\infty}^{\infty} f(y)\cos(ly)\,dy$ of (3.1.12-14) leads to

$$\frac{\partial^2 \hat{u}_T}{\partial^2 t^2} - (1+l^2)\hat{u}_T = 0, \tag{3.1.16}$$

$$\hat{u}_T(l,0) = -\hat{u}_\infty(l) = -\frac{1}{\pi}\int_{-\infty}^{\infty} e^{-|y|}\cos(ly)\,dy = -\frac{2}{\pi}\int_0^\infty \mathrm{Re}\{e^{(il-1)y}\}\,dy = -\frac{2}{\pi(1+l^2)}, \tag{3.1.17}$$

and

$$\frac{\partial \hat{u}_T(l,0)}{\partial t} = 0. \tag{3.1.18}$$

The solution to (3.1.16) subject to (3.1.17) and (3.1.18) is given by

$$\hat{u}_T = -\frac{2}{\pi(1+l^2)}\cos[\omega(l)t]$$

where $\omega(l) = (1+l^2)^{1/2}$ is the dispersion relation(2.1.27) for Poincaré waves with $w \to \infty$.

In summary

$$u(y,t) = u_\infty + u_T = e^{-|y|} - \frac{2}{\pi}\int_0^\infty \frac{1}{1+l^2}\cos[\omega(l)t]\cos(ly)\,dl \tag{3.1.19}$$

Note that $\cos[\omega(l)t]\cos(ly) = \frac{1}{2}\left[\cos(ly+\omega t)+\cos(ly-\omega t)\right]$, so that the integrand of (3.1.19) is a superposition of forward and backward propagating Poincaré waves. An alternative form of (3.1.19) that will be of use later on is

$$u(y,t) = \begin{cases} \int_0^{(t^2-y^2)^{\frac{1}{2}}} (y^2+r^2)^{-\frac{1}{2}} J_o(r)\, r\, dr & (|y|<t) \\ 0 & (|y|>t) \end{cases}, \qquad (3.1.20)$$

(Cahn, 1945).

The free surface elevation follows from (3.1.6) with $\partial/\partial x = 0$. Thus

$$\begin{aligned} \eta(y,t) &= \eta_o - \frac{\partial u}{\partial y} \\ &= \begin{cases} -1+e^{-y} & (y>0) \\ 1-e^{y} & (y<0) \end{cases} - \frac{2}{\pi}\int_0^\infty \frac{l}{(1+l^2)^{1/2}} \cos[\omega(l)t]\sin(ly)\, dl \end{aligned} \qquad (3.1.21)$$

A sketch of the developing solution with a wave front and a Poincaré wake is shown in Figure 3.1.1d.

b. The channel problem.

With the channel geometry and boundary condition the asymptotic state η_∞ now can be expected to depend on both *x* and *y*. This state is still constrained by the principle of pointwise conservation of potential vorticity (3.1.7) and one might hope to find it by solving this equation. However, doing so would require as boundary conditions the values of η_∞ along the sidewalls, and there is no clear way of anticipating these values. One is therefore forced to consider the entire problem at once.

The condition of vanishing *u* on the channel sidewalls makes a solution in terms of *u* convenient. We therefore solve (3.1.11) directly. However, *u* is identically zero in linear Kelvin waves and this approach will yield only that part of the solution due to Poincaré waves. The former will come into play when the equivalent solution for η is found.

The initial conditions:

$$u(x,y,0) = 0$$

and

$$\frac{\partial u}{\partial t}(x,y,0) = 0$$

remain the same as above. Since the initial conditions and the forcing term $(\partial\eta_o/\partial y)$ in (3.1.11) are x-independent, and since this equation has $\pm x$ symmetry, the solution will be an even function of x. Therefore a Fourier cosine series of the form

$$u(x,y,t) = \sum_{m=0}^{\infty} u_m(y,t)\cos(a_m x) \qquad (a_m = (2m+1)\pi/w,\ \ m=0,1,2,\cdots) \qquad (3.1.22)$$

is appropriate. To find u_m, multiply (3.1.11) by $2w^{-1}\cos(a_m x)$ and integrate with respect to x over the width of the channel. After several integrations by parts and application of the boundary conditions, one obtains

$$\frac{\partial^2 u_m}{\partial^2 t^2} - \frac{\partial^2 u_m}{\partial^2 y^2} + (1+a_m^2)u_m = \gamma_m \frac{d\eta_o}{dy} = -2\gamma_m \delta(y) = -2\gamma_m (1+a_m^2)^{1/2}\,\delta[(1+a_m^2)^{1/2} y] \qquad (3.1.23)$$

where $\gamma_m = \dfrac{4(-1)^m}{a_m w}$. The identity $\delta(y) = c\delta(cy)$ has been used in the final step.

Equation (3.1.23) is a forced equation for the nth Poincaré channel mode, where $n = 2m+1$. Only odd numbered modes are excited. The solution for $u_n(y,t)$ is closely related to the solution to (3.1.11) obtained in the case of an infinite domain $(\partial/\partial x = 0)$. In particular, (3.1.11) can be transformed into (3.1.23) by replacing y by $(1+a_m{}^2)^{1/2} y$, t by $(1+a_m{}^2)^{1/2} t$, and the amplitude (-2) of the forcing term by $-2\gamma_m(1+a_m^2)^{1/2}$. Since the solution to the $\partial/\partial x = 0$ version of (3.1.11) obeys the same initial conditions ($u_n(y,0)=0$) as are required here, the solution is the transformed version of (3.1.20):

$$u_m(y,t) = \gamma_m \begin{cases} \displaystyle\int_0^{(t^2-y^2)^{\frac{1}{2}}} (y^2+s^2)^{-\frac{1}{2}} J_o[(1+a_m^2)^{1/2} s]\, s\, ds & (|y| < t) \\ 0 & (|y| > t) \end{cases} \qquad (3.1.24)$$

The corresponding solution for $\eta(x,y,t)$ requires several steps and these are described in the exercises at the end of this section. The result may be written as

$$\eta(x,y,t) = K(x,y,t) + P(x,y,t) \qquad (3.1.25)$$

$$K(x,y,t) = N(y,t)\frac{\cosh(x)}{\cosh(w/2)} + V(y,t)\frac{\sinh(x)}{\cosh(w/2)} - \mathrm{sgn}(y)\left[1 - \frac{\cosh(x)}{\cosh(w/2)}\right] \qquad (3.1.26)$$

$$P(x,y,t) = -\sum_{m=0}^{\infty} (1+a_m^2)^{-1}\left[\frac{\partial u_m}{\partial y}\cos(a_m x) + a_m \frac{\partial u_m}{\partial t}\sin(a_m x)\right] \qquad (3.1.27)$$

$$N(y,t) = -\tfrac{1}{2}\left[\mathrm{sgn}(y-t) + \mathrm{sgn}(y+t)\right] \qquad (3.1.28)$$

$$V(y,t) = \tfrac{1}{2}\left[-\mathrm{sgn}(y-t) + \mathrm{sgn}(y+t)\right] \qquad (3.1.29)$$

The function $K(x,y,t)$ contains the Kelvin wave dynamics while $P(x,y,t)$ is a superposition of Poincaré modes. Consider the Kelvin waves first. The time dependence is contained in the coefficients N and V which describe step functions propagating at speeds ±1 (dimensionally $(gD)^{1/2}$, where D is the mean depth). Furthermore, N and V are exactly the surface height perturbation and velocity for the nonrotating version of this problem discussed in Section 1.2. For $w>>1$, K can be approximated as

$$K(y,t) \begin{cases} = -1 & (y > t) \\ \cong \left[2e^{(x-w/2)} - 1\right] & (0 < y < t) \\ \cong \left[-2e^{-(x+w/2)} + 1\right] & (-t < y < 0) \\ = 1 & (y < -t) \end{cases} \qquad (3.1.30)$$

The forward moving Kelvin wave therefore consists of a step that propagates along the right wall and decays inward over one Rossby radius of deformation (here unity). This wave propagates into the resting fluid (with surface elevation η=-1) and its role is to raise the elevation along the right wall to that far upstream (η=1). The wave establishes a current along the right wall that extends from y=0 to y=t. The velocity of this current is given by

$$v = \frac{\partial \eta}{\partial x} = 2e^{(x-w/2)}.$$

In addition (3.1.30) contains a backward moving Kelvin wave trapped to the left wall. This wave establishes a boundary current that carries the same volume transport (=2) as the right wall current. The current extends from y=0 to y=-t. The surface displacement along the left wall is reduced from 1 to the initial elevation (-1) of the downstream reservoir. Had we attempted to solve the problem using the semigeostrophic approximation, these Kelvin waves would have described the entire solution.

The Poincaré waves are contained in the function P. Since u_m=0 at x=±w/2, P is zero there as well and the Poincaré waves do not affect the value of η along the walls. The Kelvin waves are therefore responsible for fixing the transport of the asymptotic solution. This transport is given by

$$T = \int_{-w/2}^{w/2} v\,dx = \int_{-w/2}^{w/2} \frac{\partial \eta}{\partial x}\,dx = \eta_{w/2} - \eta_{-w/2} = 2\tanh(w/2) \qquad (3.1.31)$$

The dimensional equivalent is $T^* = 2a^* gDf^{-1}\tanh[fw^*/2(gD)^{1/2}]$, where a^*=Da. As $w = fw^*/(gD)^{1/2} \to \infty$, $T^* \to 2a^* gDf^{-1}$, also the transport of the boundary layers described above.

Despite the fact that Poincaré waves are inconsequential to the bulk transport, they are important in establishing the characteristics of the solution near y=0. In particular, they set up a jet-like flow along y=0 that carries fluid from the left wall boundary layer to the right wall boundary layer. This structure is particularly striking in the case w>>1, where (3.1.24) reduces to the cusped jet expression (3.1.13) obtained in the Rossby adjustment problem on an infinite plane. In this limit, the left-wall boundary current separates near y=0, forming a jet that crosses the channel and forms the source for the right-wall boundary current. Figure 3.2 (***a figure from Gill's book)*** shows the developing flow for the case w=4. The crossing of the flow at y=0 can clearly be seen along with the forward and backward moving Kelvin waves. The Poincaré waves lag behind the Kelvin waves due to their slower group speeds. (***I will recomputed this solution and make a better plot that shows the whole channel, the Kelvin wave fronts, and the wiggles of the Poincare′ waves.)***

Although the Poincaré waves transport no volume, they do transport energy. Calculation of the energy of the asymptotic state is somewhat involved and will not be carried out here. However it can be shown that the difference between initial and asymptotic energies per unit width of channel tend to zero as $w\to 0$, the result obtained in Section 1.2 for the nonrotating version of the problem. Here all initial energy is converted to kinetic energy and there is no wave radiation. For finite w, energy radiation occurs and the asymptotic state contains a deficit. As $w\to\infty$, this deficit approaches the value unity, as we found above for Rossby adjustment on an infinite plane.

(c) Geostrophic control

The crossing of the channel from the left to the right wall is the basis for the concept of 'geostrophic control' (Toulany and Garrett, 1984). Imagine two wide basins separated by a strait and suppose that a steady flow exists from basin A into basin B. Also assume that the dynamical setting (f-plane, horizontal bottom, homogeneous fluid, etc.) is the same as in the problem considered above. Then, if the flow is set up by the removal of a barrier that initially separates fluid of depth d_A^* in A from fluid of depth $d_B^* < d_A^*$ in B, we expect that a similar outcome will occur. The flow originating in A will be confined to a boundary current along the 'left' wall and this current will cross to the right wall within the strait and continue into basin B along that wall.

The principle of geostrophic control states that the dimensional transport between the basins is bounded by the difference in interior depths $d_A^* - d_B^*$ according to

$$T^* \le \frac{g}{2f}(d_A^{*2} - d_B^{*2}). \qquad (3.1.32)$$

The depths (or, equivalently, the layer thickness of a reduced gravity model) d_A^* and d_B^* must be measured in interior regions, away from the boundary currents. The right-hand side of (3.1.32) is the geostrophic transport of a current flowing along a horizontal

bottom with depths d_A^* and d_B^* on either side. The basic idea is that the throughflow cannot exceed the transport of the current that crosses the channel. If the depth difference is relatively small, (3.1.30) can be approximated by the linearized formula

$$T^* \cong \frac{gD}{f}(d_A^* - d_B^*), \qquad (3.1.33)$$

where D is the mean depth.

In the linearized Rossby adjustment problem we can identify the channel sectors $y<0$ and $y>0$ as basins A and B. In the limit $w \to \infty$ the predicted transport $(2gD\alpha^* f^{-1})$, is exactly given by the linearized version (3.1.33) of the bound (with $d_A^* - d_B^* = 2a^*$). In this case the geostrophic control bound gives the exact transport.

The concept of geostrophic control is most easily supported when the two basins are very wide and extend infinitely far from the separating strait. Problems arise when these conditions are not satisfied. If the upstream basin is finite, for example, the Kelvin wave that sets up the left-wall boundary current in the upstream basin would travel around the perimeter and return to the strait along the right wall, setting up a boundary flow there. Even when the basin has infinite area, ambiguities arise if its width is not large in comparison with the Rossby radius of deformation. An example is the channel adjustment problem with finite width. The upstream and downstream basins are simply the $y<0$ and $y>0$ sectors of the straight channel. The exact transport in this case is $T^* = (d_A^* - d_B^*) gDf^{-1} \tanh[\, fw^*/2(gD)^{1/2}\,]$, where d_A^* and d_B^* are to be interpreted as the *initial* surface elevations upstream and downstream of the barrier. Although it is true that this transport lies under the geostrophic control bound (3.1.33), it is the *steady* upstream values of d_A^* and d_B^*, and not the initial values, that are typically given in practical applications. Alternatively, one might interpret η_A^* and η_B^* as characteristic of the steady, upstream and downstream surface elevations of the final adjusted state. In the case of moderate channel width, however, the surface elevation varies continuously across the channel and there is no 'interior' value of d_A^* and d_B^* that characterized the surface elevation away from boundary currents.

Finally, one might also question whether the channel crossing calculated in the linear adjustment problem will persist if the full nonlinearities are retained. This topic is taken up in the next section.

Exercises

1. For the Rossby adjustment problem in an unbounded domain, calculate the final steady state without using linearization of the equations of motion. *(Probably need to give a hint here about calculating the position of the pv front.)*

2. In the limit $w>>1$, show that the velocity field set up by Poincare waves in the vacinity of $y=0$ is exactly the cusped jet found in the Rossby adjustment problem on an infinite plane. *Solution: look at the limit of (3.1.24) for finite y and infinite t.*

3. Calculation of the surface displacement $\eta(x,y,t)$ given $u(x,y,t)$. Here we follow a procedure used by Gill (1976) which exploits the fact that $u(x,y,t)$ is an even function of x.

(a) Show that (3.1.1-3.1.3 and 3.1.6) can be separated into even and odd parts as follows

$$\frac{\partial u}{\partial t} - v^{ev} = -\frac{\partial \eta^{odd}}{\partial x} \quad v^{odd} = \frac{\partial \eta^{ev}}{\partial x} \qquad (3.1.34a,b)$$

$$\frac{\partial v^{ev}}{\partial t} + u = -\frac{\partial \eta^{ev}}{\partial y} \quad \frac{\partial v^{odd}}{\partial t} = -\frac{\partial \eta^{odd}}{\partial y} \qquad (3.1.35a,b)$$

$$\frac{\partial \eta^{ev}}{\partial t} + \frac{\partial v^{ev}}{\partial y} = 0 \quad \frac{\partial \eta^{odd}}{\partial t} + \frac{\partial u}{\partial x} + \frac{\partial v^{odd}}{\partial y} = 0 \qquad (3.1.36a,b)$$

$$\frac{\partial v^{odd}}{\partial x} - \frac{\partial u}{\partial y} - \eta^{ev} = -\eta_o \quad \frac{\partial v^{ev}}{\partial x} = \eta^{odd} \qquad (3.1.37a,b)$$

where $\eta = \eta^{ev} + \eta^{odd}$, $\eta^{ev} = \frac{1}{2}[\eta(x,y,t) + \eta(-x,y,t)]$, and $\eta^{odd} = \frac{1}{2}[\eta(x,y,t) - \eta(-x,y,t)]$, and similar decompositions apply to u and v.

(b) From the result in (a) show that

$$\frac{\partial^2 \eta^{ev}}{\partial x^2} - \eta^{ev} = \frac{\partial u}{\partial y} - \eta_o$$

$$\frac{\partial^2 v^{ev}}{\partial x^2} - v^{ev} = -\frac{\partial u}{\partial t}$$

Show that the general solutions to these equations can be expressed as

$$\eta^{ev}(x,y,t) = -\sum_{m=0}^{\infty} \frac{\gamma_m \,\mathrm{sgn}(y) + \partial u_m / \partial y}{(1+a_m^2)} \cos(a_m x) + N(y,t)\frac{\cosh(x)}{\cosh(w/2)} \qquad (3.1.38)$$

and

$$v^{ev}(x,y,t) = \sum_{m=0}^{\infty} \frac{\partial u_m / \partial t}{(1+a_m^2)} \cos(a_m x) + V(y,t)\frac{\cosh(x)}{\cosh(w/2)} \qquad (3.1.39)$$

where again $\gamma_m = (2m+1)\pi / w$.

(c) Show that the functions N and V can be determined through substitution of these last solutions into (3.1.35a) and (3.1.36a) leading to

$$\frac{\partial V}{\partial t} + \frac{\partial N}{\partial y} = 0 \quad \text{and} \quad \frac{\partial N}{\partial t} + \frac{\partial V}{\partial y} = 0 \qquad (3.1.40)$$

(d) From the results of (b) show that an initial condition on V is $V(y,0)=0$ whereas $N(y,0)$ is determined by the relation

$$-\mathrm{sgn}(y) = -A(x)\,\mathrm{sgn}(y) + N(y,0)\frac{\cosh(x)}{\cosh(w/2)}$$

where

$$A(x) = \sum_{m=0}^{\infty} \frac{\gamma_m \cos(a_m x)}{(1+a_m^2)}. \qquad (3.1.41)$$

To help evaluate $A(x)$, use the above series to show that

$$\frac{d^2A}{dx^2} - A = -\sum_{m=0}^{\infty} \gamma_m \cos(a_m x) = -1.$$

From this equation and from the boundary conditions $A(w/2)=A(-w/2)=0$, which follow from (3.1.41), deduce that $A = 1 - \dfrac{\cosh(x)}{\cosh(w/2)}$ and therefore $N(y,0) = -\mathrm{sgn}(y)$. From (3.1.40) and the initial conditions just described, deduce the solutions (3.1.28) and (3.1.29).

(e) Finally, show using (3.1.37b) that

$$\eta^{odd} = -\sum_{m=0}^{\infty} \frac{a_m}{(1+a_m^2)} \frac{\partial u_m}{\partial t} \sin(a_m x)$$

Figures

3.1 (a): Initial condition for Rossby adjustment problem. (b) and (c): Interface elevation and velocity $u(y)$ for $t\to\infty$ state on infinite plane. (d): Radiation of Poincaré waves at t=?? as computed from (3.1.21).

3.2 Contours of surface elevation for the linear Rossby adjustment problem in channel with w=4 at t=4. The contour values range from -.9 to +.9 in even increments as the channel is crossed. (Constructed from Figure 10.7 in Gill, 1982).

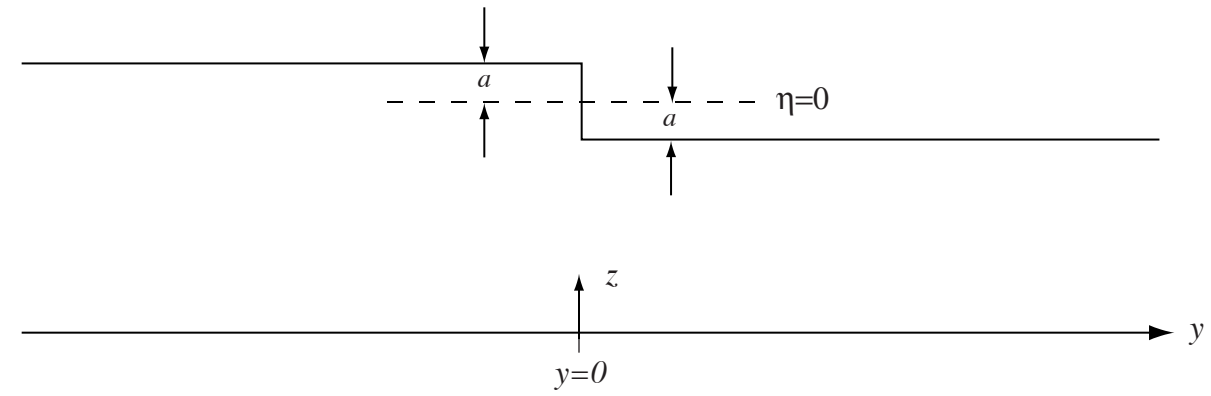

(a)

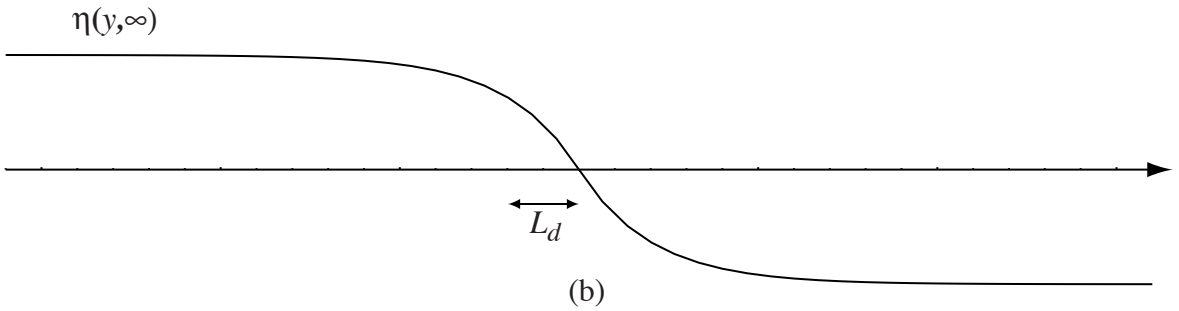

(b)

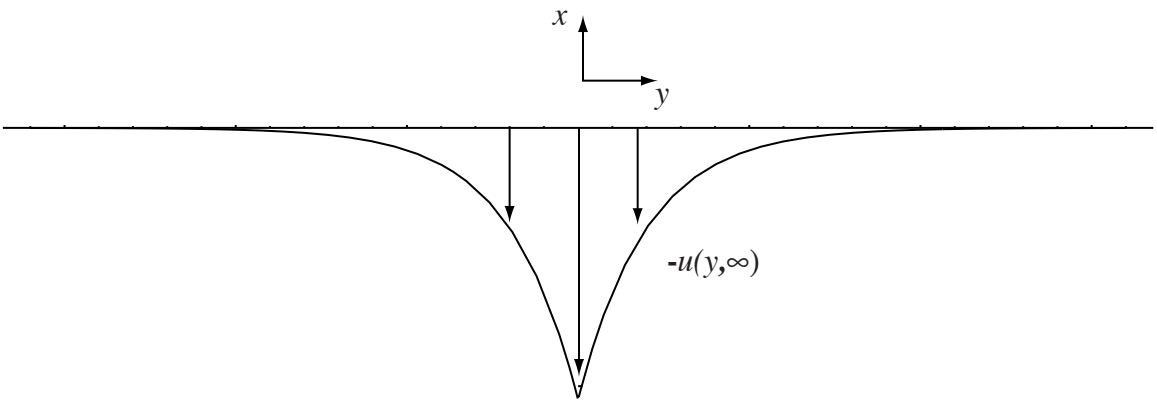

(c)

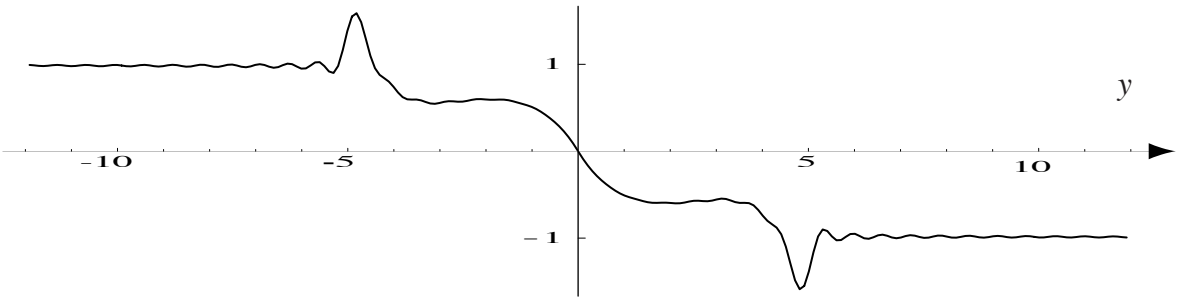

(d)

Figure 3.1

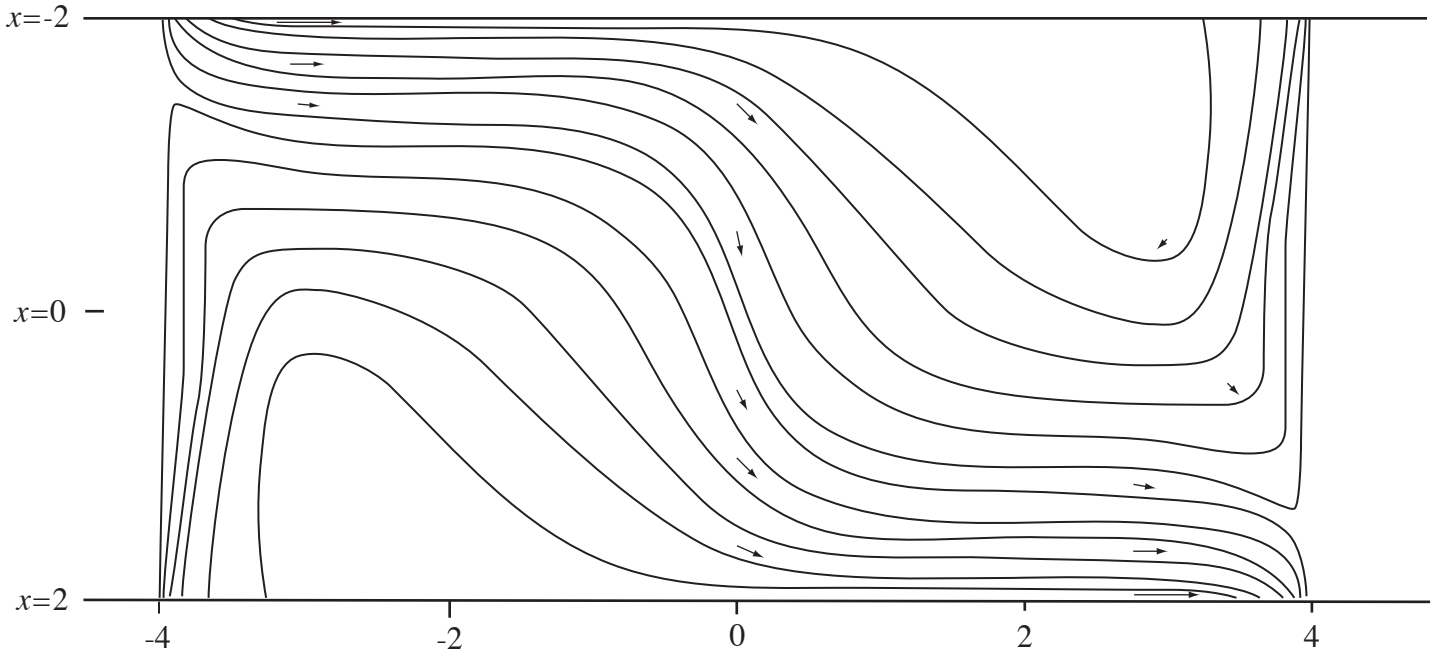

Figure 3.1.2